# Reactions of Laser-Ablated Iron Atoms with Oxygen Molecules: Matrix Infrared Spectra and Density Functional Calculations of OFeO, FeOO, and Fe($O_2$)

**Lester Andrews,*,† George V. Chertihin,† Alessandra Ricca,‡ and Charles W. Bauschlicher, Jr.‡**

*Contribution from the Department of Chemistry, University of Virginia, Charlottesville, Virginia 22901, and STC-230-3, NASA Ames Research Center, Moffett Field, California 94035*

*Received October 2, 1995*⊗

**Abstract:** Reactions of laser-ablated Fe atoms and $O_2$ molecules in argon condensing on a 10 K surface have produced sharp infrared absorptions at 1204.5, 945.6, and 797.1 $cm^{-1}$ that are identified as FeOO and OFeO, respectively, through the use of isotopic substitution and DFT structure and isotopic frequency calculations. Annealing to 30 and 50 K produced a strong 956.0-$cm^{-1}$ band, which is due to cyclic Fe($O_2$); visible photolysis destroyed the 1204.5-$cm^{-1}$ FeOO band, but it was regenerated on annealing. Formation of the more stable dioxo insertion product OFeO requires activation energy whereas the superoxo and peroxo addition products FeOO and Fe($O_2$) can be formed on diffusion of cold reagents in solid argon. The FeOO spectrum observed and calculated here compares favorably with those reported for oxyhemoproteins, which provides further support for the Fe−O−O binding geometry in these biologically important metalloproteins.

## Introduction

Iron may be the most significant metal in materials, chemistry and biology, and the reaction of iron and oxygen is certainly of great practical importance. While the simple and fundamental reaction atomic Fe + molecular $O_2$ has been examined in argon matrices,[1−3] in the gas phase[4−6] and by theoretical calculations,[6−8] the initial reaction mechanisms and product identities and structures are far from understood. The straightforward products FeOO, open OFeO, and cyclic Fe($O_2$) have all been considered.[1−3] The superoxo FeOO species is a simple and important model compound for the binding of dioxygen in hemoproteins.[9−12] The dioxo OFeO species is analogous to OTiO and is of structural interest as a member of the transition metal dioxide OMO series.[13,14] Finally, the peroxo Fe($O_2$) molecule is related to other side-bound dioxygen species such as Li($O_2$), Ca($O_2$), and Ni($O_2$) where the degree of charge transfer is an important question.[15−17]

Ground state iron atoms are unreactive with $O_2$ in the gas phase near room temperature presumably because of the need for third-body collisions to remove the reaction exothermicity. However, electronically excited iron atoms are expected to be more reactive and perhaps required to form the (more stable) higher oxidation state dioxo product OFeO. Recent matrix isolation experiments with pulsed-laser ablated Be, Mg, Ca, B, Al, Ga, Ti, Zr, and Hf atoms have shown that many of the ablated atoms contain the excess kinetic/electronic energy required to activate insertion reactions.[13,16,18−22] Hence, pulsed-laser ablated Fe atoms were reacted with $O_2$ in a condensing argon stream, and DFT calculations were done to identify the primary product molecules, structures, and spectra, and to understand the mechanism of this important reaction.

## Experimental Section

Iron (Johnson Matthey, 99.98%) atoms were evaporated by pulsed 1064 nm radiation (10−20 mJ/pulse at the sample) and codeposited with Ar/$O_2$ samples using methods described previously.[18−22] FTIR spectra were recorded on a Nicolet 750 spectrophotometer at 0.5 $cm^{-1}$ resolution and ±0.1 $cm^{-1}$ accuracy.

## Results and Discussion

Infrared spectra are shown for the reaction of Fe atoms and 1% $O_2$ in argon in the 1240−740 $cm^{-1}$ region (Figure 1a). New

---

† University of Virginia.

‡ NASA Ames Research Center.

⊗ Abstract published in *Advance ACS Abstracts,* December 15, 1995.

(1) Abramowitz, S.; Acquista, N.; Levin, I. W. *Chem. Phys. Lett.* **1977**, *50*, 423.

(2) Chang, S.; Blyholder, G.; Fernandez, J. *Inorg. Chem.* **1981**, *20*, 2813.

(3) Serebrennikov, L. V. *Vestn. Mosk. Univ. Ser. 2, Khim.* **1988**, *29*, 451. Serebrennikov, L. V. Sc.D. Thesis, Moscow State University, 1990, Moscow.

(4) Whetten, R. L.; Cox, D. M.; Trevor, D. J.; Kaldor, A. *J. Phys. Chem.* **1984**, *89*, 566.

(5) Mitchell, S. A.; Hackett, P. A. *J. Chem. Phys.* **1990**, *93*, 7822.

(6) Helmer, M.; Plane, J. M. C. *J. Chem. Soc., Faraday Trans.* **1994**, *90*, 395.

(7) Blyholder, G.; Head, J.; Ruette, F. *Inorg. Chem.* **1982**, *21*, 1539.

(8) Lyne, P. D.; Mingos, D. M. P.; Ziegler, T.; Downs, A. J. *Inorg. Chem.* **1993**, *32*, 4785.

(9) Watanabe, T.; Ama, T.; Nakamoto, K. *J. Phys. Chem.* **1984**, *88*, 440.

(10) Potter, W. T.; Tucker, M. P.; Houtchens, R. A.; Caughey, W. S. *Biochemistry* **1987**, *26*, 4699.

(11) Hirota, S.; Ogura, T.; Appleman, E. H.; Shinzawa-Itah, K.; Yoshikawa, S.; Kitagawa, T. *J. Am. Chem. Soc.* **1994**, *116*, 10564 and references therein.

(12) Hirota, S.; Ogura, T.; Kitagawa, T. *J. Am. Chem. Soc.* **1995**, *117*, 821.

(13) Chertihin, G. V.; Andrews, L. *J. Phys. Chem.* **1995**, *99*, 6356.

(14) Van Zee, R. J.; Hamrick, Y. M.; Weltner, W., Jr. *J. Phys. Chem.* **1992**, *96*, 7247.

(15) Andrews, L. *J. Chem. Phys.* **1969**, *50*, 4288.

(16) Andrews, L.; Yustein, J. T.; Thompson, C. A.; Hunt, R. D. *J. Phys. Chem.* **1994**, *98*, 6514.

(17) Huber, H.; Klotzbucher, W.; Ozin, G. A.; Vander Voet, A. *Can. J. Chem.* **1973**, *51*, 2722.

(18) Burkholder, T. R.; Andrews, L. *J. Chem. Phys.* **1991**, *95*, 8697.

(19) Andrews, L.; Burkholder, T. R.; Yustein, J. T. *J. Phys. Chem.* **1992**, 96, 10182.

(20) Burkholder, T. R.; Yustein, J. T.; Andrews, L. *J. Phys. Chem.* **1992**, *96*, 10189.

(21) Andrews, L.; Yustein, J. T. *J. Phys. Chem.* **1993**, *97*, 12700.

(22) Thompson, C. A.; Andrews, L. *J. Chem. Phys.* **1994**, *100*, 8689.

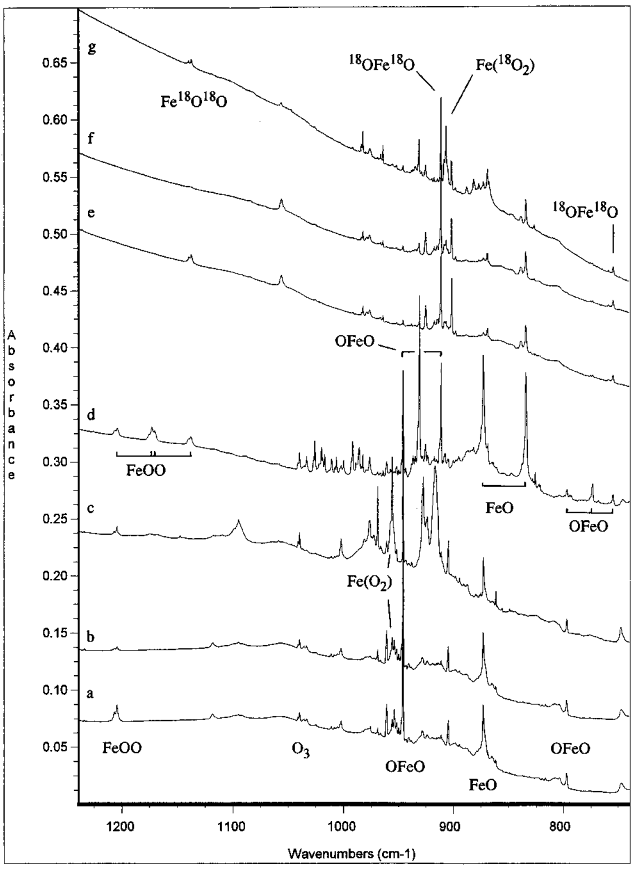

**Figure 1.** Infrared spectra in the 1240−740 cm$^{-1}$ region for pulsed-laser ablated Fe atoms codeposited with 1% $O_2$ in argon during condensation at 10 K: (a) 2 h deposition with $^{16}O_2$, (b) after 30 min glower photolysis with $\lambda > 630$ nm filter, (c) after annealing to 40 K with source blocked, (d) 2 h deposition with $^{16,18}O_2$, (e) 3 h deposition with $^{18}O_2$, (f) after 30 min glower photolysis, and (g) after annealing to 30 K with source blocked.

bands are noted at 1204.5 (labeled FeOO), 945.8, and 797.1 (labeled OFeO), and 872.8 cm$^{-1}$ (labeled FeO);[23] additional bands at 660.6 and 517.4 cm$^{-1}$ are due to $Fe_2O_2$ isomers as will be discussed in an analysis of all of the observed bands.[24] Photolysis (Figure 1b) using the glower source and a $\lambda > 630$ nm pass filter almost destroyed the 1204.5 cm$^{-1}$ band and slightly increased a weak 956.0 cm$^{-1}$ band with little effect on the other absorptions. Annealing to 50 K (Figure 1c) regenerated part of the 1204.5 cm$^{-1}$ band, produced a strong 956.0 cm$^{-1}$ band and other absorptions for higher oxides, and decreased the 945.8 and 797.1 cm$^{-1}$ bands. Reaction with scrambled $^{16,18}O_2$ (Figure 1d) gave significant isotopic multiplets that will be discussed for each molecule below. Finally, reaction with $^{18}O_2$ gave a displaced product spectrum (Figure 1e) and important diagnostic 16/18 ratios that are listed in Table 1. Exposure of the 10 K sample to the Nicolet 750 infrared source (Figure 1f) destroyed the 1137.6 cm$^{-1}$ counterpart band, but annealing to 30 K (Figure 1g) *in the dark* regenerated the band and produced a strong 906.7 cm$^{-1}$ absorption.

Density functional theory (DFT) calculations were performed on the three isomers OFeO, $Fe(O_2)$, and FeOO using the hybrid B3LYP functional;[25] triplet and quintet states were considered. The Fe basis set is a [8s 4p 3d] contraction of the primitive set of Wachters;[26] the s and p spaces are contracted using the number 3, while the d space is contracted (311). Two diffuse p functions are added to describe the 4p orbital which are the functions of Wachters multiplied by 1.5; diffuse s and p functions (α(s) = 0.013963 and α(p) = 0.02092), the d function,[27] and an f polarization function (α = 1.339) are added. The O basis set 6-311+G(2df) was employed.[28] Geometries were optimized and harmonic frequencies were computed using the "finegrid" option in Gaussian 92/DFT;[29] results are summarized in Table 2. The OFeO cations and anions were also calculated, but no convincing evidence was found for these ions.

**Table 1.** Isotopic Frequencies (cm$^{-1}$) Observed for Iron Oxide Species in Solid Argon

| $^{16}O_2$ | $^{18}O_2$ | $^{16,18}O_2$ | $R(^{16}O/^{18}O)$ | anneal[a] | assignment |
|---|---|---|---|---|---|
| 1496.5 | 1424.8 | | 1.0503 | ++ | $(\nu_1 + \nu_2)$ $Fe(O_2)$ |
| 1494.6 | 1423.1 | 1457 | 1.0502 | | site |
| 1204.5 | 1137.6 | 1204.5, 1173.0, 1170.4, 1137.6 | 1.0588 | + | FeOO |
| 956.0 | 906.7 | 956.0, 931.2, 906.7 | 1.0544 | ++ | $\nu_1$ $Fe(O_2)$ |
| 957.7 | 908.2 | 957.7, 933.1, 908.2 | 1.0545 | | site |
| 945.8 | 911.2 | 945.8, 930.9, 911.2 | 1.0380 | − | $(\nu_3)$ $O^{56}FeO$ |
| 951.8 | 917.4 | 951.8, 936.7, 917.4 | 1.0375 | − | $(\nu_3)$ $O^{54}FeO$ |
| 872.8 | 834.5 | 872.8, 834.5 | 1.0459 | − | $^{56}FeO$ |
| 876.2 | 838.2 | 876.2, 838.2 | 1.0453 | − | $^{54}FeO$ |
| 797.1 | 754.8 | 797.1, 773.7, 754.8 | 1.0560 | − | $(\nu_1)$ OFeO |
| 661.5 sh | 632.8 | 661.6, 639.5, 632.8, 681.1 | 1.0454 | 0 | OFeFeO |
| 660.6 | 631.9 | 660.6, 638.7, 631.9, 680.3 | 1.0454 | 0 | OFeFeO |
| 548.4 | 524.8 | | 1.0450 | ++ | $(\nu_2)$ $Fe(O_2)$ |
| 547.3 | 523.9 | | 1.0447 | | |
| 517.4 | 494.8 | 517.4, 508.1, 494.8 | 1.0457 | − | $(\nu_5)$ $(FeO)_2$ |

[a] Annealing behavior up to 50 K.

**Table 2.** Isotopic Frequencies (cm$^{-1}$) Calculated for the Ground State OFeO, $Fe(O_2)$, and FeOO Structural Isomers Using the B3LYP Functional

| | 16−16 | 16−18 | 18−18 |
|---|---|---|---|
| OFeO[a] | 958.3 (91)[d] | 945.7 | 922.3 |
| $^3B_1$ | 891.3 (25) | 862.4 | 844.2 |
| | 194.3 (29) | 190.4 | 186.4 |
| $Fe(O_2)$[b] | 842.9 (132) | 821.8 | 799.7 |
| $^5A_1$ | 509.7 (3) | 499.7 | 488.2 |
| | 462.1 (2) | 449.1 | 438.0 |
| FeOO[c] | 1159.8 (185) | 1128.2, 1126.0 | 1093.3 |
| $^3A''$ | 472.7 (21) | 453.3, 471.5 | 452.2 |
| | 134.7 (2) | 132.4, 130.4 | 128.3 |

[a] Geometry: Fe−O = 1.582 Å, ∠O−Fe−O = 141.5°. [b] Geometry: Fe−O = 1.812 Å, O−O = 1.491 Å. [c] Geometry: Fe−O = 1.869 Å, O−O = 1.306 Å, ∠Fe−O−O = 114.8°. [d] Infrared intensities (km/mol).

The sharp 945.8 and 797.1 cm$^{-1}$ bands maintain a constant 11/1 relative intensity in over 20 experiments under a range of laser powers and oxygen concentrations. Both bands exhibited triplet absorptions with scrambled isotopic oxygen indicating *two equivalent oxygen atoms*. The sharp 951.8 cm$^{-1}$ satellite band intensity is appropriate for the $^{54}Fe$ in natural abundance and it denotes the participation of a *single iron atom*. The 16/

---

(23) Green, D. W.; Reedy, G. T. *J. Mol. Spectrosc.* **1979**, *78*, 257 and references therein.

(24) Chertihin, G. V.; Saffel, W.; Yustein, J. T.; Andrews, L.; Neurock, M.; Ricca, A.; Bauschlicher, C. W., Jr. *J. Phys. Chem.* To be published.

(25) Stevens, P. J.; Devlin, F. J.; Chablowski, C. F.; Frisch, M. J. *J. Phys. Chem.* **1994**, *98*, 11623.

(26) Wachters, A. J. H. *J. Chem. Phys.* **1970**, *52*, 1033.

(27) Hay, P. J. *J. Chem. Phys.* **1977**, *66*, 4377.

(28) Frisch, M. J.; Pople, J. A.; Binkley, J. S. *J. Chem. Phys.* **1984**, *80*, 3265.

(29) Gaussian 92/DFT, Revision G.2, Frisch, M. J.; Trucks, G. W.; Schlegel, H. B.; Gill, P. M. W.; Johnson, B. G.; Wong; M. W.; Foresman, J. B.; Robb, M. A.; Head-Gordon, M.; Replogle, E. S.; Gomperts, R.; Andres, J. L.; Raghavachari, K.; Binkley, J. S.; Gonzalez, C.; Martin, R. L.; Fox, D. J.; Defrees, D. J.; Baker, J.; Stewart, J. J. P.; Pople, A. J., Gaussian, Inc.: Pittsburgh, PA, 1993.

18 isotopic ratios 1.0380 and 1.0560 are characteristic of the $\nu_3$ (antisymmetric) and $\nu_1$ (symmetric) modes of a symmetrical, bent OFeO molecule. In fact the 16/18 and 54/56 isotopic $\nu_3$ ratios define 158 ± 5° upper and 144 ± 5° lower limits, respectively, for the OFeO angle; the average value (150 ± 10°) provides a measure of the OFeO valence angle.[13,30] Although DFT calculations with the B3LYP functional predict a $^5B_2$ state for OFeO at slightly lower energy (−2.42 kcal/mol), the calculated valence angle (118°) for the $^5B_2$ state is not compatible with experiment; however, the valence angle (142°) calculated for the $^3B_1$ state is in agreement. Similar bond angles were calculated with the Becke−Perdew functional, but the $^5B_2$ state was predicted to be slightly higher (2.35 kcal/mol) in energy than the $^3B_1$ state. Clearly, the $^5B_2$ and $^3B_1$ states are close in energy and experimental measurements must be used to identify the ground OFeO state.

The criterion for state determination is agreement between calculated and observed 16/18 ratios as a description of the normal modes for the OFeO states. Both functionals predict 16/18 ratios for the $^3B_1$ state of OFeO in excellent agreement with the observed $\nu_3$ and $\nu_1$ isotopic 16/18 frequency ratios, 1.0380 and 1.0560, respectively; B3LYP isotopic ratios for $\nu_3$ and $\nu_1$ are 1.0390 and 1.0558, respectively. On the other hand both functionals predict incompatible 16/18 ratios for the $^5B_2$ state of OFeO; B3LYP isotopic ratios for $\nu_3$ and $\nu_1$ are 1.0416 and 1.0511, respectively. The comparison between theory and experiment for frequency match to identify ground state molecules must include isotopic frequencies.

The 1204.5 $cm^{-1}$ band is destroyed by visible radiation, but annealing to 30 K *in the dark* allows regeneration of the band. The band exhibited a quartet at 1204.5, 1173.0, 1170.4, and 1137.6 $cm^{-1}$ with scrambled isotopic oxygen identifying the stretching vibration of *two inequivalent oxygen atoms* (16/18 = 1.0588). The lower energy calculated for $^3A''$ FeOO in spite of the known preference of B3LYP for higher spin states due to mixing in Hartree−Fock exchange shows that the ground FeOO state is indeed $^3A''$. Note the strong band calculated at 1159.8 $cm^{-1}$ for FeOO and the 2.2 $cm^{-1}$ separation (Table 2) calculated for this mode with Fe 16−18 and Fe 18−16 isotopes, which are in excellent agreement with experimental values (Table 1) and confirm this assignment to FeOO.

The 956.0 $cm^{-1}$ band grows markedly on annealing, and the scrambled isotopic experiment reveals a triplet for *two equivalent oxygen atoms*. The 16/18 ratio 1.0544 for this $\nu_1$ mode is intermediate between pure O−O and Fe−$O_2$ stretching values. A much weaker band at 548.4 $cm^{-1}$ with 16/18 ratio 1.0450 is due to the $\nu_2$ mode where both $\nu_1$ and $\nu_2$ modes are mixtures of symmetric O−O and Fe−$O_2$ stretching internal coordinates as defined by the 16/18 ratios. Confirmation of this assignment and identification of cyclic Fe($O_2$) is found in the observation of a weak $\nu_1 + \nu_2$ combination band with the appropriate 16/18 ratio (Table 1). DFT/B3LYP calculations predict the $^5A_1$ state lower (−6.1 kcal/mol) than the $^3B_2$ state, and the normal mode analysis as defined by 16/18 frequency ratios gives an excellent match with experiment for the $^5A_1$ state, but not for the $^3B_2$ state. The 16/18 frequency ratios calculated for the triplet state $\nu_1$ and $\nu_2$ modes, 1.0594 and 1.0388, do not agree with the experimental values, 1.0544 and 1.0447, as do the 1.0540 and 1.0440 ratios calculated for the quintet state of Fe($O_2$). At the same level of theory, the $^7A_1$ state is calculated 1.5 kcal/mol below the $^5A_1$ state. However, the frequencies calculated for the $^7A_1$ state (1157 ($a_1$), 401 ($a_1$), 398 ($b_2$)) are not even close to agreement with experiment. Clearly, the B3LYP bias toward higher spin states results in the $^7A_1$ state being calculated too low in energy. Hence, cyclic Fe($O_2$) is identified as the $^5A_1$ state.

There is interest in the trend in valence angle as a function of the number of valence electrons for symmetrical BAB triatomic molecules analogous to the Walsh treatment, but emphasizing d instead of p orbitals on the central atom.[13,14,31−33] It has been predicted that such triatomics will change from bent to linear with the 19th valence electron.[14] However, OFeO with 20 valence electrons is bent (150 ± 10°). The bent structure is stabilized by oxygen in-plane $\pi$ lone pair donation to the Fe $\delta$-like orbital. This donation is forbidden by symmetry in the linear molecule.

The vibrational spectroscopy of $O_2$ bound to Fe in oxyhemoproteins is difficult to perform and interpret, but it has been thoroughly studied in many model compounds.[9−12] Recent work reveals oxygen isotope sensitive bands assigned to a $\nu$(O−O) mode in the 1160−1100 $cm^{-1}$ range, $\nu$(Fe−OO) near 570 $cm^{-1}$, and $\delta$(Fe−O−O) near 425 $cm^{-1}$.[11] The 1204.5 $cm^{-1}$ band observed here for $\nu$(O−O) in FeOO is displaced some 40−100 $cm^{-1}$ less from isolated $O_2$ than $O_2$ bound in oxyhemoproteins. Clearly, the complexing porphyrin and histidine ligands in hemoglobin provide charge density to Fe(II) for more reduction of $O_2$ than naked Fe can provide. The $\nu$(Fe−$O_2$) and $\delta$(Fe−O−O) modes calculated here (Table 2) for FeOO further show that naked Fe binds superoxo dioxygen less strongly than Fe(II) in hemoproteins. Note that the 114.8° Fe−O−O angle calculated here is in excellent agreement with that measured by X-ray diffraction for myoglobin (115°) but not for hemoglobin (153, 159°).[34,35]

The cyclic Fe($O_2$) peroxo species is not in fact a true peroxide as the 956.0 $cm^{-1}$ frequency is not as low as the 736 $cm^{-1}$ value for Ca($O_2$)[16] and the Raman fundamental for ionic peroxides[36] although the calculated O−O bond length in Fe($O_2$) is in the peroxide range. The net charge on Fe in $^5A_1$ Fe($O_2$) is calculated to be +0.69. The analogous Ni($O_2$) species exhibits a similar 966 $cm^{-1}$ fundamental.[17]

The oxidative insertion reaction 1 requires activation energy as OFeO is formed in high yield only on deposition of laser ablated Fe atoms with $O_2$; DFT calculations predict that the insertion reaction is exothermic by 64 kcal/mol.

$$\mathrm{Fe} + \mathrm{O_2} \xrightarrow{E_a} (\mathrm{OFeO})^* \xrightarrow[\text{relax}]{} \mathrm{OFeO} \qquad \text{calcd } \Delta E = -64 \text{ kcal/mol} \quad (1)$$

$$\mathrm{Fe} + \mathrm{O_2} \xrightarrow{E_a} (\mathrm{OFeO})^* \rightarrow \mathrm{FeO} + \mathrm{O} \qquad \text{calcd } \Delta E = +22 \text{ kcal/mol} \quad (2)$$

It is possible that metastable $^5P_3$ atoms produced by laser ablation are responsible for the insertion reaction.[37,38] Although some FeO is produced here from decomposition of energized OFeO, a substantial amount of the OFeO product is quenched and trapped by the matrix.

The superoxo addition product FeOO is formed during deposition of energetic Fe atoms and $O_2$, but the cyclic peroxo addition product Fe($O_2$) is not formed with dilute $O_2$ until annealing in the solid matrix.

---

(30) Allavena, M.; Rysnik, R.; White, D.; Calder, V.; Mann, A. E. *J. Chem. Phys.* **1969**, *50*, 3399.

(31) Walsh, A. D. *J. Chem. Soc.* **1953**, 2266.

(32) Hayes, E. F. *J. Phys. Chem.* **1966**, *70*, 3740.

(33) Weltner, W., Jr. *Ber. Bunsen-Ges. Phys. Chem.* **1978**, *82*, 80.

(34) Phillips, S. E. V. *Nature* **1978**, *273*, 247; *J. Mol. Biol.* **1980**, *142*, 531.

(35) Shaanan, B. *Nature* **1982**, *296*, 683; *J. Mol. Biol* **1983**, *171*, 31.

(36) Evans, J. C. *J. Chem. Soc., Chem. Commun.* **1969**, 682.

(37) Cellucci, T. A.; Nixon, E. R. *J. Phys. Chem.* **1985**, *89*, 1991.

(38) Chertihin, G. V.; Andrews, L. *J. Phys. Chem.* **1995**, *99*, 12131.

$$\mathrm{Fe} + \mathrm{O_2} \rightarrow \mathrm{FeOO} \qquad \text{calcd } \Delta E = -17 \text{ kcal/mol} \tag{3}$$

$$\mathrm{Fe} + \mathrm{O_2} \rightarrow \mathrm{Fe(O_2)} \qquad \text{calcd } \Delta E = -27 \text{ kcal/mol} \tag{4}$$

This is probably a consequence of different collision dynamics and quenching of the reaction exothermicity during deposition and on annealing in the solid matrix. Although FeOO is calculated to be a higher energy species than $Fe(O_2)$ by some 10 kcal/mol, FeOO can be quenched through the low frequency bending mode more effectively than $Fe(O_2)$, and as a result FeOO is stabilized here during deposition of energetic Fe atoms and $O_2$ molecules in excess argon. However, on annealing the surrounding matrix cage can efficiently quench the cyclic $Fe(O_2)$ formed. Although annealing in the dark does produce some FeOO, the major band growth is due to the more stable cyclic $Fe(O_2)$ species where the matrix cage provides little steric hinderance to formation of the more stable cyclic species. Both FeOO and $Fe(O_2)$ are formed on diffusion and reaction of ground state Fe and $O_2$ in solid argon.

In hemoglobin, the Fe(II) site is coordinated to four nitrogen lone pairs from the porphyrin ring system and one nitrogen lone pair from one histidine side chain. Apparently, the availability of only one more coordination site to bind dioxygen to Fe(II) in the stable octahedral coordinating structure in hemoglobin favors the formation of the superoxo Fe−OO linkage over the more strongly bound cyclic peroxo species $Fe(O_2)$. The spectra of FeOO and $Fe(O_2)$ are shown here to be distinctly different. The FeOO spectrum observed and calculated here compares favorably with spectra reported for oxyhemoproteins,[10−12] which provides strong support for the Fe−O−O binding geometry in these biologically important metalloproteins.

**Acknowledgment.** We acknowledge support for this research from NSF Grant No. CHE 91-22556, an NRC Fellowship for A.R., and helpful discussions with S. H. Andrews, A. S. Brill, and H. Frei.

JA953338F